Carcinogenesis vol.31 no.5 pp.911–917, 2010
doi:10.1093/carcin/bgp221
Advance Access publication December 11, 2009

Myricetin inhibits UVB-induced angiogenesis by regulating PI-3 kinase *in vivo*

Sung Keun Jung[1,2,3,†], Ki Won Lee[2,†], Sanguine Byun[1,2,3], Eun Jung Lee[1], Jong-Eun Kim[1,3], Ann M.Bode[3], Zigang Dong[3,*] and Hyong Joo Lee[1]

[1]Major in Biomodulation, Department of Agricultural Biotechnology, Seoul National University, Seoul 151-742, Republic of Korea, [2]Bio/Molecular Informatics Center, Department of Bioscience and Biotechnology, Konkuk University, Seoul 143-701, Republic of Korea and [3]The Hormel Institute, University of Minnesota, 801 16th Avenue Northeast, Austin, MN 55912, USA

[*]To whom correspondence should be addressed. Tel: +1 507 437 9600; Fax: +1 507 437 9606;
Email: zgdong@hi.umn.edu
Correspondence may also be addressed to Hyong Joo Lee.
Tel: +82 2 880 4860; Fax: +82 2 873 5095;
Email: leehyjo@snu.ac.kr

Myricetin is one of the principal phytochemicals in onions, berries and red wine. Previous studies showed that myricetin exhibits potent anticancer and chemopreventive effects. The present study examined the effect of myricetin on ultraviolet (UV) B-induced angiogenesis in an SKH-1 hairless mouse skin tumorigenesis model. Topical treatment with myricetin inhibited repetitive UVB-induced neovascularization in SKH-1 hairless mouse skin. The induction of vascular endothelial growth factor, matrix metalloproteinase (MMP)-9 and MMP-13 expression by chronic UVB irradiation was significantly suppressed by myricetin treatment. Immunohistochemical and western blot analyses revealed that myricetin inhibited UVB-induced hypoxia inducible factor-1α expression in mouse skin. Western blot analysis and kinase assay data revealed that myricetin suppressed UVB-induced phosphatidylinositol-3 (PI-3) kinase activity and subsequently attenuated the UVB-induced phosphorylation of Akt/p70^{S6K} in mouse skin lysates. A pull-down assay revealed the direct binding of PI-3 kinase and myricetin in mouse skin lysates. Our results indicate that myricetin suppresses UVB-induced angiogenesis by regulating PI-3 kinase activity *in vivo* in mouse skin.

Introduction

Angiogenesis, defined as the sprouting of new blood vessels, is a crucial part of cancer development (1,2). During the prevascular phase of tumor growth, tumors cannot exceed 1–2 mm in diameter. Through angiogenesis, however, tumors are able to grow beyond this size and metastasize to other organs (3). Therefore, various anti-angiogenic strategies are currently being tested in clinical trials and are anticipated to provide promising results in cancer treatment. Of the various targets being considered for therapeutic intervention against angiogenesis, interfering with cell signaling related to the release of major growth factors and proteolytic enzymes such as vascular endothelial growth factor (VEGF) and matrix metalloproteinases (MMPs) is one of the major approaches to suppress cancer tissue angiogenesis (4). An *in vivo* study using transgenic mice showed that the upregulation of VEGF expression in the epidermis stimulated skin vascularization and increased the number of tortuous and hyperpermeable blood vessels (5). MMPs are not only involved in tumor progression, invasion and progression but are also required for angiogenesis (6).

Abbreviations: ATP, adenosine triphosphate; ERK, extracellular signal-regulated kinase; HIF-1, hypoxia inducible factor-1; MEK, mitogen-activated protein kinase kinase; MMP, matrix metalloproteinase; PI-3, phosphatidylinositol-3; UV, ultraviolet; VEGF, vascular endothelial growth factor.

[†]These authors contributed equally to this work.

VEGF and MMPs are regulated by the heterodimeric transcription factor hypoxia inducible factor-1 (HIF-1), which acts as a key regulator of the hypoxic response and plays a crucial role in angiogenesis (7–9). Among the HIF-α subunits, HIF-1α is ubiquitously expressed and has a major role in regulating oxygen homeostasis and tumor formation (10,11). Previous studies have shown that HIF-1α activity is regulated by activation of the phosphatidylinositol-3 (PI-3) kinase/Akt signal transduction pathway (12). Moreover, ultraviolet (UV) light-induced PI-3 kinase/Akt signaling was recently shown to result in enhanced HIF-1α and VEGF expression (13,14). Therefore, the inhibition of angiogenesis through the suppression of HIF-1α by targeting PI-3 kinase signaling may prove to be a promising strategy for cancer therapy and chemoprevention.

Multiple lines of evidence have suggested that naturally occurring phytochemicals in the human diet are excellent chemopreventive agents (15); hence, they may also be potent angiopreventive agents or angiogenic inhibitors. Myricetin (3,3′,4′,5,5′,7-hexahydroxyflavone) is a major flavonoid found in a number of foods, including onions, berries, grapes and red wine (16–18). Previous studies have shown that myricetin has antioxidant, anti-inflammatory and anticancer effects (17–20). In addition, myricetin was shown to inhibit 12-*O*-tetradecanolyphorbol-13-acetate-induced MMP-2 activity by suppressing protein kinase C translocation, extracellular signal-regulated kinases (ERKs) phosphorylation and c-Jun protein expression (21). Myricetin strongly inhibits neoplastic cell transformation and mouse skin carcinogenesis by targeting mitogen-activated protein kinase kinase (MEK) and Fyn, respectively (20,22). These data indicate that myricetin is a potent chemopreventive agent, but the underlying *in vivo* mechanism and targets of the anti-angiogenic effects of myricetin are unclear. Here, we report that myricetin strongly inhibited ultraviolet (UV) B-induced abnormal vascularization in a long-term mouse skin model. Myricetin suppressed UVB-induced PI-3 kinase activity and subsequently attenuated UVB-induced HIF-1α, VEGF and MMPs expression in mouse dorsal skin *in vivo*.

Materials and methods

Materials

Myricetin (95%) was purchased from Sigma–Aldrich (St Louis, MO). Antibodies against HIF-1α and MMP-13 were obtained from Novous Biologicals (Littleton, CO) and Chemicon International (Temecula, CA), respectively. Antibodies against phosphorylated Akt (Ser473), total Akt, phosphorylated p70^{S6K} (Thr389), total p70^{S6K}, phosphorylated MEK (Ser217/221) and total MEK were purchased from Cell Signaling Technology (Beverly, MA). Antibodies against VEGF, MMP-9, phosphorylated ERK (Thr202/Tyr204) and total ERK were obtained from Santa Cruz Biotechnology (Santa Cruz, CA). cyanogen bromide–Sepharose 4B, glutathione–Sepharose 4B, [γ-^{32}P] adenosine triphosphate (ATP) and the chemiluminescence detection kit were purchased from GE Healthcare (Piscataway, NJ). The protein assay kit was obtained from Bio-Rad (Hercules, CA).

Animals

The animal study and protocol were approved by the Institute of Laboratory Animal Resources, Seoul National University (Seoul, Korea). SKH-1 hairless mice (6 weeks of age; mean body weight, 25 g) were also purchased from the Institute of Laboratory Animal Resources, Seoul National University. The animals were stabilized for 1 week prior to the study and had free access to food and water. The animals were housed in climate-controlled quarters (24°C at 50% humidity) with a 12 h light–12 h dark cycle.

UVB irradiation

UVB irradiation was performed using a UVB irradiation system. The spectral peak of the UVB source (Bio-Link Crosslinker, Vilber Lourmat, Torcy, France) was at 312 nm. The mice were divided into four groups containing 15 animals each: one control group, one UVB-treated group and two myricetin-treated groups. The mice in the control group were treated topically with 200 μl of acetone, whereas those in the UVB group were treated topically with 200 μl of acetone prior to UVB (0.18 J/cm^2) exposure for 27 weeks. The mice in the third and fourth groups were treated topically with myricetin in acetone 60 min prior

to UVB (0.18 J/cm^2) irradiation for 27 weeks. The frequency of irradiation was set at three times per week. The respective doses of myricetin (8 or 20 nmol in 200 µl of acetone) and UVB (0.18 J/m^2) were applied to the dorsal area.

Preparation of the skin lysates

The mice were treated topically on the dorsal skin surface with myricetin (8 or 20 nmol in 200 µl of acetone) 1 h prior to UVB irradiation and were euthanized 24 h after the last UVB treatment for further study. To isolate the proteins, the dorsal mouse skin was excised and fat was removed on ice. The samples were immediately pulverized in liquid nitrogen using a mortar and pestle. The pulverized skin was then homogenized on ice using an Ika Works T 10 basic homogenizer (Staufen im Breisgau, Germany) and the proteins were extracted with a 20% sodium dodecyl sulfate solution containing the protease inhibitor phenylmethylsulfonyl fluoride (1 mM; Calbiochem, La Jolla, CA), 10 mM iodoacetamide, 1 mM leupeptin, 1 mM antipain, 0.1 mM Na_3VO_4 and 5 mM sodium fluoride. The lysates were centrifuged at 12 000 r.p.m. for 20 min, and the protein content was determined using a protein assay kit (Bio-Rad).

Western blotting

For western blot analysis, 100 µg of each mouse skin extract, comprising both epidermal and dermal portions of the skin, was subjected to 10% sodium dodecyl sulfate–polyacrylamide gel electrophoresis and transferred to a polyvinylidene difluoride membrane (GE Healthcare). After blotting, the membrane was incubated overnight with a primary antibody at 4°C. All protein bands were visualized using a chemiluminescence detection kit (Amersham Pharmacia Biotech, Piscataway, NJ) after hybridization with a horseradish peroxidase-conjugated secondary antibody. The relative amount of protein associated with each antibody was quantified using Image J (National Institutes of Health, Bethesda, MD).

Gelatin zymography

Gelatin zymography was used to assess the gelatinolytic activity of MMP-9. The protein content was determined using a Bio-Rad protein assay kit. Equal amounts of protein extract were then mixed with non-reducing sample buffer, incubated for 15 min at room temperature and subjected to 12% sodium dodecyl sulfate–polyacrylamide gel electrophoresis using gels containing 1 mg/ml gelatin. After electrophoresis, the gels were washed twice with 2.5% Triton X-100 for 30 min, rinsed three times for 30 min with a 50 mM Tris–HCl buffer (pH 7.6) containing 5 mM $CaCl_2$, 0.02% Brij-35 and 0.2% sodium azide and incubated overnight at 37°C. The gels were then stained with a 0.5% Coomassie Brilliant Blue R-250 solution containing 10% acetic acid and 20% methanol for 30 min and destained with a 7.5% acetic acid solution containing 10% methanol. Areas of gelatinase activity were detected as clear bands against the blue background. The amount of protein present in each band was determined (from JPEG images) by densitometric analysis using Image J (National Institutes of Health).

Immunohistochemical analysis

Dorsal skin from the mice was prepared for immunohistochemical analysis of HIF-1α expression. Sections (5 µm thick) of 10% neutral formalin solution-fixed paraffin-embedded tissues were cut on silane-coated glass slides and then deparaffinized three times with xylene and dehydrated through a graded alcohol bath. The deparaffinized sections were incubated in 20 µg/ml proteinase K for 20 min at room temperature for antigen retrieval. To prevent non-specific staining, each section was treated with 3% hydrogen peroxide for 20 min and a blocking solution containing 1% bovine serum albumin for 2 h. For the detection of the target protein, the slides were incubated overnight with an affinity-purified primary antibody at 4°C in 1% bovine serum albumin and then developed using an anti-rabbit or anti-mouse Histostain Plus Kit (Zymed Laboratories, South San Francisco, CA). Peroxidase-binding sites were detected by staining with 3,3′-diaminobenzidine tetrahydrochloride (Sigma–Aldrich). Mayer's hematoxylin was applied as a counterstain (Sigma–Aldrich).

In vivo PI-3 kinase immunoprecipitation and kinase assay

UVB-induced PI-3 kinase activation was detected in accordance with the instructions provided by Upstate Biotechnology (Milford, MA). In brief, excised proteins were extracted with lysis buffer [20 mM Tris–HCl (pH 7.4), 1 mM ethylenediaminetetraacetic acid, 150 mM NaCl, 1 mM ethyleneglycol-bis(aminoethylether)-tetraacetic acid, 1% Triton X-100, 1 mM β-glycerophosphate, 1 mg/ml leupeptin, 1 mM Na_3VO_4 and 1 mM phenylmethylsulfonyl fluoride] and then centrifuged at 14 000 r.p.m. for 15 min. In advance, 700 µg of mouse skin extract were mixed with protein A/G beads (20 µl) for 1 h at 4°C and then centrifuged at 12 000 r.p.m. for 1 min at 4°C. The supernatant fraction was then mixed with an antibody to detect phosphatidylinositol (20 µl) and rocked gently overnight at 4°C. The immunoprecipitates were then incubated with reaction buffer [100 µM *N*-2-hydroxyethylpiperazine-*N*′-2-ethanesulfonic acid (pH 7.6), 50 µM $MgCl_2$ and 250 µM ATP containing 10 µCi of [γ-^{32}P] ATP for an additional 10 min at 30°C. The reaction was stopped by adding 15 µl of 4 N HCl and 130 µl of chloroform:methanol (1:1). After vortexing, 20 µl of the lower chloroform phase was spotted onto a 1% potassium oxalate-coated silica gel plate that had been previously activated for 1 h at 110°C. The resulting ^{32}P-labeled PI-3-phosphate was separated by thin layer chromatography and the radiolabeled spots were visualized by autoradiography.

Preparation of myricetin–Sepharose 4B

Sepharose 4B beads (0.3 g) were suspended in 1 mM HCl and coupling solution [0.1 M $NaHCO_3$ (pH 8.3) and 0.5 M NaCl] and mixed. Myricetin (1–2 mg) was mixed with the solution and then, the preparation of Sepharose 4B beads were added to the myricetin mixture. The myricetin–Sepharose 4B beads were then rotated end-over-end overnight at 4°C. The medium was subsequently transferred to 0.1 M Tris–HCl buffer (pH 8.0) and again rotated end-over-end overnight at 4°C. Finally, the medium was washed three times with a 0.1 M acetate buffer (pH 4.0) containing 0.5 M NaCl followed by a wash with 0.1 M Tris–HCl (pH 8.0) containing 0.5 M NaCl.

Pull-down assays

For the *in vivo* pull-down assays, dorsal skin from the control and myricetin-treated mice was prepared as described for western blotting and the proteins were extracted as described above for the PI-3 kinase immunoprecipitation and kinase assays. A total of 500 µg of each mouse skin extract was incubated with myricetin–Sepharose 4B (or Sepharose 4B alone as a control) beads (100 µl, 50% slurry) in reaction buffer [50 mM Tris (pH 7.5), 5 mM ethylenediaminetetraacetic acid, 150 mM NaCl, 1 mM dithiothreitol, 0.01% Nonidet P-40, 2 µg/ml bovine serum albumin, 0.02 mM phenylmethylsulfonyl fluoride and 1 µg of a protease inhibitor mixture]. The beads were then washed and the proteins bound to the beads were analyzed by western blotting as described above.

Statistical analysis

When appropriate, the data are expressed as means ± SEMs and significant differences were determined using one-way analysis of variance (23). A probability value of $P < 0.05$ was used as the criterion for statistical significance. All analyses were performed using Statistical Analysis Software (SAS, Cary, NC).

Results

Myricetin inhibits UVB-induced neovascularization in the skin of SKH-1 hairless mice

Given that angiogenesis is a promising target for cancer prevention and treatment (1,2,10,21,22), we investigated the effect of myricetin on UVB-induced angiogenesis using dorsal skin from mice exposed to UVB (0.18 J/cm^2) irradiation three times a week for 27 weeks. Myricetin inhibited chronic UVB-induced blood vessel formation in the skin of the mice (Figure 1). These results indicate that UVB-induced neovascularization is attenuated by myricetin.

Myricetin suppresses UVB-induced VEGF expression in SKH-1 hairless mouse skin

Because VEGF has been suggested as a primary pro-angiogenic agent (2,6,21,24), we evaluated the effect of myricetin on UVB-induced VEGF expression in SKH-1 hairless mouse skin. Western blot analysis revealed that myricetin significantly inhibited UVB-induced VEGF expression (Figure 2A) by 81 and 89% ($P < 0.05$ and $P < 0.01$ compared with the UVB-irradiated group; $n = 3$) at 8 and 20 nmol in 200 µl of acetone, respectively (Figure 2B). Both sets of results indicated that UVB-induced VEGF expression in mouse skin is significantly inhibited by myricetin.

Myricetin attenuates UVB-induced MMP-9 and -13 expressions in SKH-1 hairless mouse skin

The upregulation of MMPs is essential for irregular new blood vessel formation (25,26); thus, we next determined the effect of myricetin on the UVB-induced upregulation of MMP-9 and -13. Topical administration of myricetin significantly inhibited the UVB-induced upregulation of pro- and active-MMP-9 by 66 and 43% at 8 nmol and 67 and 58% at 20 nmol ($P < 0.05$ compared with the UVB-irradiated group; $n = 3$) in 200 µl of acetone, respectively (Figure 3A). Similarly, myricetin significantly inhibited the UVB-induced upregulation of MMP-13 by 82 and 90% ($P < 0.05$ and $P < 0.01$ compared with the UVB-treated group; $n = 3$) at 8 and 20 nmol in 200 µl of acetone,

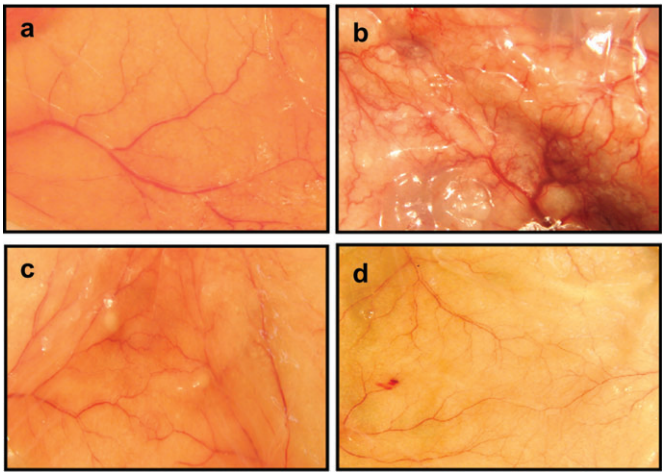

Fig. 1. Effects of myricetin on UVB-induced blood vessel formation in SKH-1 hairless mice. Myricetin inhibits UVB-induced neovascularization in SKH-1 hairless mouse skin. (**a**) Vehicle-treated controls, (**b**) UVB-irradiated (0.18 J/cm^2) mice and UVB plus (**c**) mice treated with 8 nmol myricetin or (**d**) mice treated with 20 nmol myricetin. Fifteen mice were treated topically with myricetin (8 or 20 nmol in 200 µl of acetone/mouse) or vehicle as described in Materials and Methods and then irradiated with UVB light 3× a week for 27 weeks. Photographs of blood vessels in the mice were taken after euthanization at the end of the experiment using a Samsung digital camera.

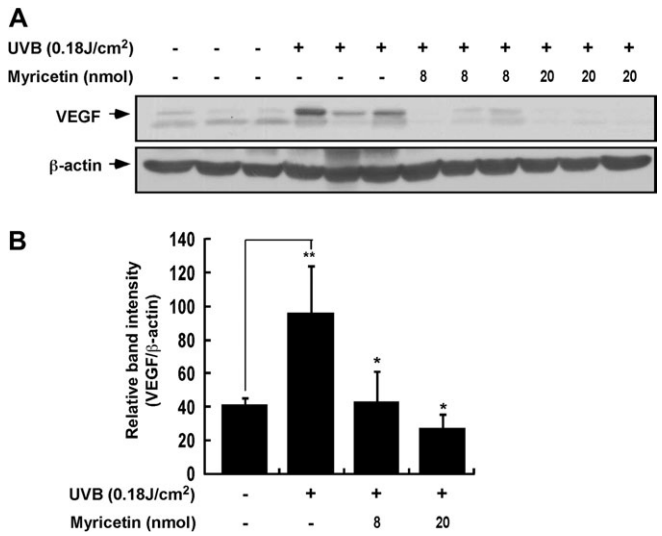

Fig. 2. The effect of myricetin on UVB-induced VEGF expression in SKH-1 hairless mice. (**A** and **B**) Myricetin significantly inhibits UVB-induced VEGF expression in SKH-1 hairless mice. VEGF or β-actin expression was assessed by western blotting using antibodies against VEGF or β-actin as described in Materials and Methods. (B) Each band was densitometrically quantified by image analysis. The results are shown as means ± SEMs ($n = 3$). The pound (#) symbol indicates a significant difference ($P < 0.05$) between the control group and the UVB-treated group, whereas the asterisk (*) indicates a significant difference ($P < 0.05$) between the UVB-irradiated/myricetin-treated and UVB-only irradiated groups.

respectively (Figure 3B). Thus, the UVB-induced upregulation of MMP-9 and -13 in mouse skin is strongly attenuated by myricetin treatment.

Myricetin represses UVB-induced HIF-1α expression in SKH-1 hairless mouse skin

HIF-1 is a key regulator of several angiogenic factors, including VEGF and MMPs (2,7,25,27,28); thus, we investigated the effect of

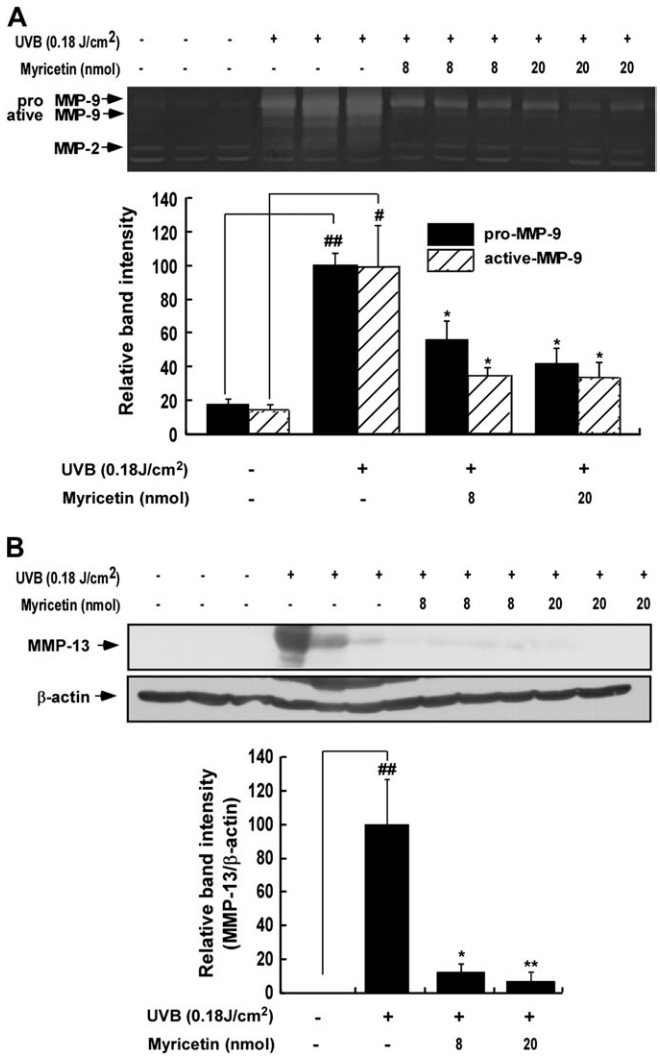

Fig. 3. Effects of myricetin on UVB-induced MMP-9 activity and MMP-13 expression in SKH-1 hairless mice. (**A**) Myricetin inhibits UVB-induced MMP-9 activity in SKH-1 hairless mice. Proteins were extracted from isolated mouse skin samples as described in Materials and Methods. MMP-9 activity was assessed by gelatin zymography as described in Materials and Methods. (**B**) Myricetin inhibits UVB-induced MMP-13 expression in SKH-1 hairless mice as shown by western blotting using antibodies against MMP-13 or β-actin. Each band was densitometrically quantified by image analysis. The results are shown as means ± SEMs ($n = 3$). The pound (# and ##) symbols indicate a significant difference ($P < 0.05$ and $P < 0.01$, respectively) between the control and UVB-irradiated groups, whereas the asterisks (* and **) indicate a significant difference ($P < 0.05$ and $P < 0.01$, respectively) between the UVB-irradiated/myricetin-treated and UVB-only irradiated groups.

myricetin on UVB-induced HIF-1α expression in SKH-1 hairless mice. We found that UVB-induced HIF-1α expression was reduced by myricetin in SKH-1 hairless mouse skin (Figure 4A). Western blotting revealed that myricetin suppressed UVB-induced HIF-1α expression by 88 and 89% ($P < 0.05$ compared with the UVB-irradiated group; $n = 3$) at 8 and 20 nmol in 200 µl of acetone, respectively (Figure 4B).

Myricetin inhibits the UVB-induced phosphorylation of Akt, p70^{S6K}, MEK and ERKs in SKH-1 hairless mouse skin

Because the PI-3 kinase pathway functions in the regulation of HIF-1α, we investigated the effect of myricetin on Akt and p70^{S6K}. Western blotting showed that myricetin inhibited the UVB-induced phosphorylation of Akt by 86 and 94% ($P < 0.05$ compared with the UVB-irradiated group; $n = 5$) at 8 and 20 nmol in 200 µl of acetone,

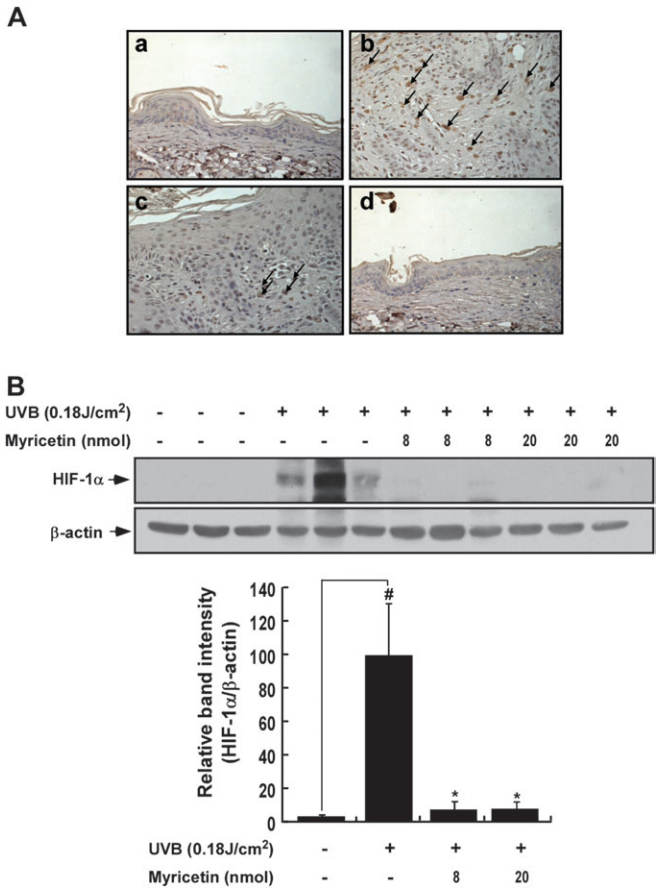

Fig. 4. Effects of myricetin on UVB-induced HIF-1α expression in SKH-1 hairless mice. (**A** and **B**) Myricetin inhibits UVB-induced HIF-1α expression in SKH-1 hairless mice. (**a**) Vehicle-treated controls, (**b**) UVB-irradiated (0.18 J/cm^2) mice and mice treated with UVB plus (**c**) 8 nmol of myricetin or (**d**) 20 nmol of myricetin. The mice were treated as described in Figure 1B. Serial sections were mounted on silane-coated slides and immunostained for HIF-1α as described in Materials and Methods. The photos are representative of results from five or six tissue samples. HIF-1α appears brown. HIF-1α or β-actin expression was assessed by western blotting as described in Materials and Methods. Each band was densitometrically quantified by image analysis. The results are shown as means ± SEMs ($n = 3$). The pound (#) symbol indicates a significant difference ($P < 0.05$) between the control and UVB-irradiated groups, whereas the asterisk (*) indicates a significant difference ($P < 0.05$) between the UVB-irradiated/myricetin-treated and UVB-only irradiated groups.

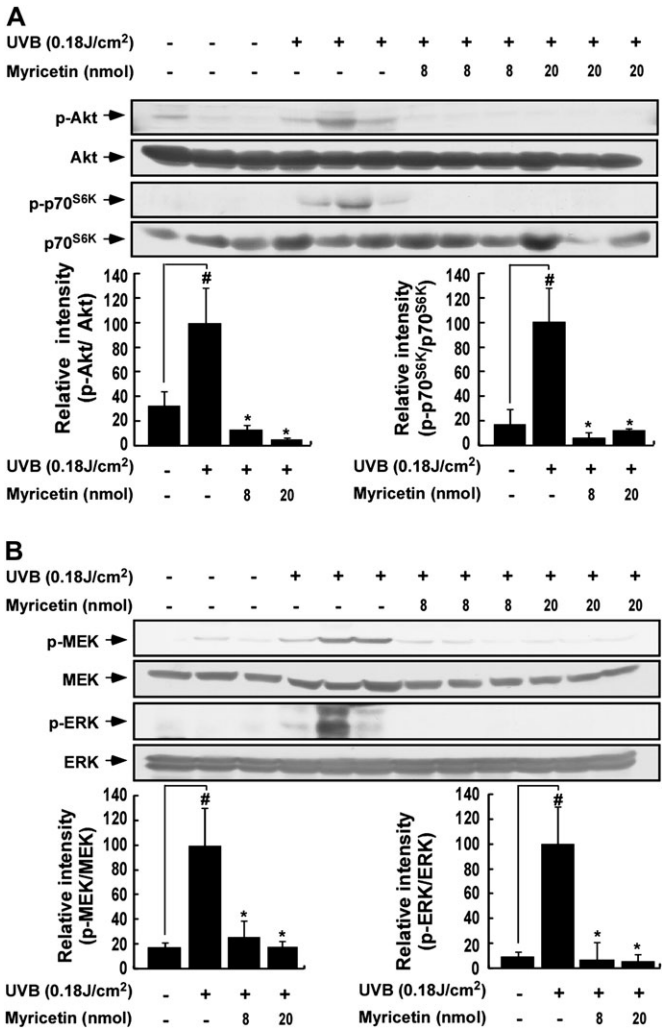

Fig. 5. Effect of myricetin on UVB-mediated signaling in SKH-1 hairless mouse skin. (**A**) Myricetin inhibits the phosphorylation of Akt and p70^{S6K} in SKH-1 hairless mouse skin. (**B**) Myricetin inhibits the UVB-induced phosphorylation of MEK and ERKs in SKH-1 hairless mouse skin. Proteins were extracted from isolated mouse skin samples as described in Materials and Methods. The phosphorylation of Akt, p70^{S6K}, MEK and ERKs and level of total Akt, p70^{S6K}, MEK and ERKs was assessed by western blotting. The results are shown as means ± SEMs ($n = 3$). The pound (#) symbol indicates a significant difference ($P < 0.05$) between the control and UVB-irradiated groups, whereas the asterisk (*) indicates a significant difference ($P < 0.05$) between the UVB-irradiated/myricetin-treated and UVB-only irradiated groups.

respectively (Figure 5A). Myricetin also inhibited the UVB-induced phosphorylation of p70^{S6K} by 93 and 87% ($P < 0.05$ compared with the UVB-irradiated group; $n = 3$) at 8 and 20 nmol in 200 µl of acetone, respectively (Figure 5A). Previous studies showed that angiogenesis is regulated by the MEK/ERKs signaling pathway (29,30). Therefore, we used western blotting to analyze the effect of myricetin on ERKs signaling. Myricetin inhibited the UVB-induced phosphorylation of MEK by 74 and 82% ($P < 0.05$ compared with the UVB-irradiated group; $n = 3$) at 8 and 20 nmol in 200 µl of acetone, respectively. Myricetin also inhibited the UVB-induced phosphorylation of ERKs by 94 and 95% ($P < 0.05$ compared with the UVB-irradiated group; $n = 5$) at 8 and 20 nmol in 200 µl of acetone, respectively (Figure 5B). These data indicate that myricetin inhibits UVB-induced phosphorylation of Akt/p70S6K and MEK/ERKs signaling.

Myricetin attenuates UVB-induced PI-3 kinase activity in SKH-1 hairless mouse skin

We next examined the effect of myricetin on PI-3 kinase activity because myricetin substantially inhibited the phosphorylation of Akt. PI-3 kinase activity was significantly suppressed by myricetin in SKH-1 hairless mice (Figure 6A). We performed a pull-down assay to determine whether myricetin interacts directly with PI-3 kinase in mouse skin extracts. In skin lysates, PI-3 kinase bound myricetin–Sepharose 4B beads (Figure 6B, lane 3) but not plain Sepharose 4B beads (Figure 6B, lane 2). Thus, myricetin inhibits UVB-induced PI-3 kinase activity by binding with PI-3 kinase in SKH-1 mouse skin.

Discussion

Aberrant angiogenesis occurs in many skin cancers. In tumors, transformed lesions are able to grow to a certain size, but growth is restricted due to limited oxygen diffusion. To expand this limit, all tumors depend on angiogenesis (31). Like other tumors, skin tumors are highly angiogenic, and increased angiogenesis in skin cancer has

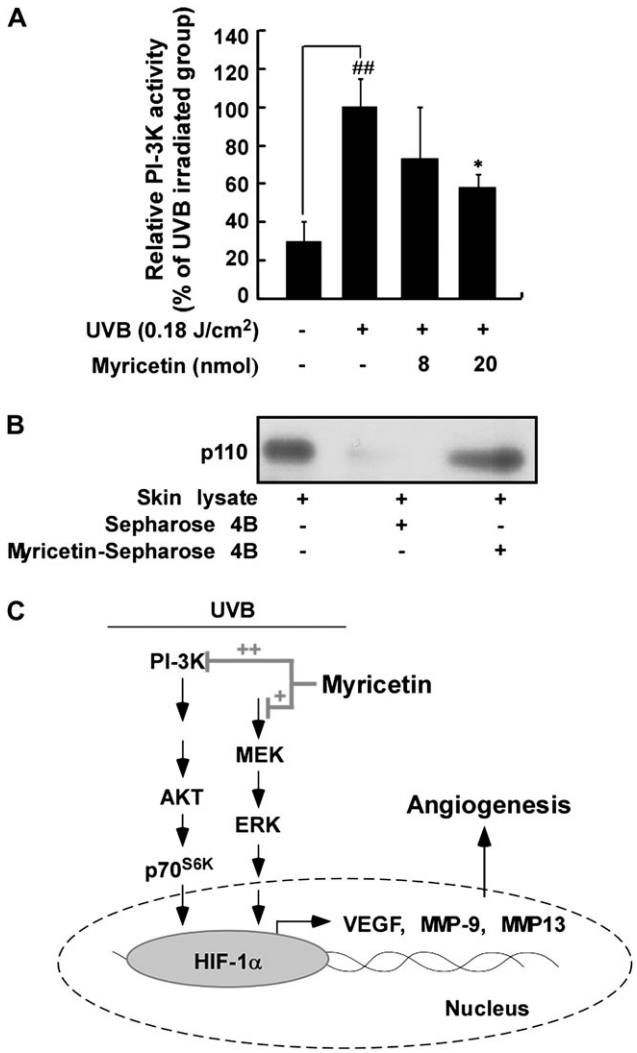

Fig. 6. Effect of myricetin on UVB-induced PI-3 kinase activity in SKH-1 hairless mice. (**A**) Myricetin inhibits UVB-induced PI-3 kinase activity in a dose-dependent manner. To assay for PI-3 kinase activity, dorsal skin lysates were prepared from the epidermis and subjected to immunoprecipitation and a PI-3 kinase assay as described in Materials and Methods. The results are shown as means ± SEMs ($n = 3$). The pound (##) symbols indicate a significant difference ($P < 0.01$) between the control and UVB-irradiated groups; the asterisk (*) indicates a significant difference ($P < 0.05$) between the UVB-irradiated/myricetin-treated and UVB-irradiated groups. (**B**) Myricetin binds PI-3 kinase directly in mouse skin lysates. *In vivo* myricetin binding was confirmed by immunoblotting using an antibody against subunit p110: lane 1 (input control), whole lysate from mouse dorsal skin; lane 2 (control), mouse dorsal skin lysate precipitated with Sepharose 4B beads (see Materials and Methods) and lane 3, whole-cell lysate from mouse dorsal skin precipitated by myricetin–Sepharose 4B affinity beads (see Materials and Methods). (**C**) Simplified view of the proposed anti-angiogenic mechanism of myricetin.

been well documented. Increased microvessel density compared with normal skin has been reported in actinic keratosis and squamous cell carcinoma (30). Other studies have confirmed a rise in angiogenesis in squamous cell carcinoma (32) and basal cell carcinoma has shown an increase in angiogenesis compared with normal skin (33).

Since the critical role of angiogenesis in tumor growth was established, many cancer treatment strategies have been developed with the goal of suppressing angiogenesis. Several antagonists to angiogenic growth factors and receptors are currently being tested in clinical trials, including gefitinib (Iressa®) and erlotinib (Tarceva®) for squamous cell carcinoma and sorafenib (Nexavar®), bevacizumab (Avastin®) and erlotinib (Tarveca®) for melanoma. Additionally, other substances have been discovered to disrupt angiogenic signaling in skin cancer, such as inhibitors of COX-2, hedgehog signaling, mammalian target of rapamycin, Toll-like receptor and growth factors (34). Anti-angiogenic agents may exert their chemopreventive effects by blocking or retarding the development of blood vessels during tumorigenesis (35).

A previous study showed that myricetin inhibited 7,12-dimethylbenz(*a*)-anthracene, benzo[*a*]pyrene and *N*-methyl-*N*-nitrosourea-induced tumor formation in a skin tumorigenesis model (36). A recent study suggested myricetin as a chemopreventive agent because of its inhibitory effect on mammalian thioredoxin reductase (19). In a two-stage carcinogenesis model and JB6 P+ cell system, we showed that myricetin strongly inhibited neoplastic cell transformation and mouse skin carcinogenesis by targeting MEK and Fyn, respectively (20,22). Together, these results suggest that myricetin may be an effective chemopreventive agent, but its direct molecular targets and mechanisms of anti-angiogenesis have not been fully clarified. We found that chronic UVB irradiation induces angiogenesis in the skin of SKH-1 hairless mice but that the process can be inhibited by myricetin treatment. These results indicate that chronic UVB irradiation induces neovascularization in SKH-1 hairless mouse skin but that it might be prevented by myricetin.

In pathological angiogenesis, tumors release large amounts of angiogenic activators. Various angiogenic mediators, including VEGF, fibroblast growth factor, interleukin-8 and placenta growth factors, are known to be overexpressed in melanoma (37,38). VEGF is a major mediator of pathological angiogenesis (8,9), and the loss of one *VEGF* allele causes severe disruption of embryonic blood vessel formation (39). Moreover, VEGF-null embryonic stem cells are markedly impaired in their tumor formation ability, which indicates that VEGF is critical for tumorigenesis and angiogenesis (40). In this study, we found that myricetin substantially inhibited UVB-induced VEGF expression in mouse skin, which indicates that myricetin has the ability to retard angiogenesis *in vivo*. MMPs have been shown to stimulate angiogenesis (2,8), and our present data indicate that myricetin has a significant inhibitory effect on the expression of MMP-9 and -13. The expression of matrix-degrading proteinases, including MMP-9 and -13, is necessary for remodeling of the extracellular matrix to facilitate the formation of new blood vessels (41). MMP-9 is a component of an angiogenic switch that makes VEGF available for interaction with its receptors (42). During angiogenesis, several MMPs, gelatinases and membrane-type 1 MMP play important roles in the degradation of the basement membrane and prevascular components of the extracellular matrix, the modulation of angiogenic factors and the production of endogenous angiogenic inhibitors (43). The role of MMP-9 as a crucial target in anti-angiogenesis was demonstrated in a previous study showing that interleukin-10, an angiogenic inhibitor, suppressed primary human prostate cell-induced angiogenesis by stimulating tissue inhibitor of metall opeptidase inhibitor 1, a tissue metalloproteinase inhibitor, and inhibited MMP-9 expression (44).

HIF-1α is a major mediator of angiogenesis whose target genes include *VEGF* (2,9) and *MMPs* (28). HIF-1α regulates MMP-9 in patients with non-small-cell lung cancer (45). In HIF-$1\alpha^{-/-}$ mouse embryonic stem cells, tumor growth was significantly decreased because of reduced angiogenesis (11). A recent report revealed that HIF-1 overexpression is associated with an increase in the death rate from many types of cancer and that the suppression of HIF-1 is effective in tumor repression (46). In this study, increased HIF-1α expression in response to chronic irradiation was inhibited by myricetin treatment. Previous studies showed that HIF-1 synthesis is regulated by the activation of PI-3 kinase (12,47,48) and ERKs signaling (29,49). In particular, recent data indicate that HIF-1α or VEGF expression is upregulated by UV and arsenite-induced PI-3 kinase signaling (13,30). Myricetin suppressed the UVB-induced phosphorylation of Akt/$p70^{S6K}$ and MEK/ERKs in SKH-1 hairless mouse skin lysates. We previously showed that myricetin significantly suppressed UVB-induced Fyn kinase activity and subsequent Raf/MEK/ERKs signaling. Thus, the inhibition of MEK/ERKs signaling by myricetin

in mouse skin could be mediated through a reduction in Fyn kinase activity (22). According to our results, myricetin also inhibits UVB-induced Akt/p70^{S6K} signal transduction; therefore, the molecular target of myricetin for the inhibition of UVB-induced HIF-1α expression might be PI-3 kinase. Our kinase and pull-down assay results showed that myricetin inhibits UVB-induced PI-3 kinase activity directly by binding with PI-3 kinase. A previous X-ray crystallographic study indicated that myricetin attenuates PI-3 kinase activity by fitting into the ATP-binding pocket of PI-3 kinase (50); however, no evidence exists for a direct interaction between myricetin and PI-3 kinase *in vivo*. Our results are the first to demonstrate that myricetin attenuates UVB-induced HIF-1α expression and suppresses the UVB-induced phosphorylation of Akt by regulating PI-3 kinase activity *in vivo* in mouse skin.

Collectively, myricetin significantly inhibits UVB-induced neovascularization in the skin of SKH-1 hairless mice. The anti-angiogenic effect of myricetin is due to its ability to block HIF-1α expression by directly inhibiting PI-3 kinase activity, suggesting that PI-3 kinase is a critical target of myricetin in the inhibition of VEGF and MMPs expression in SKH-1 hairless mouse skin. This novel function of myricetin may lead to clinical advances in the anti-angiogenic treatment of skin cancer.

Funding

World Class University program (R31-2008-00-10056-0) through the Korea Science and Engineering Foundation, the Ministry of Education, Science and Technology; BioGreen 21 Program (20070301-034-042 and 027), Rural Development Administration; The Hormel Foundation and National Institutes of Health (CA077646, CA111536, CA120388, ES016548).

Acknowledgements

Priority Research Centers program (2009–0093824).

Conflict of Interest Statement: None declared.

References

1. Folkman,J. (1995) Seminars in Medicine of the Beth Israel Hospital. Boston. Clinical applications of research on angiogenesis. *N. Engl. J. Med.*, **333**, 1757–1763.
2. Bergers,G. *et al*. (2003) Tumorigenesis and the angiogenic switch. *Nat. Rev. Cancer*, **3**, 401–410.
3. Carmeliet,P. *et al*. (2000) Angiogenesis in cancer and other diseases. *Nature*, **407**, 249–257.
4. Liekens,S. *et al*. (2001) Angiogenesis: regulators and clinical applications. *Biochem. Pharmacol.*, **61**, 253–270.
5. Detmar,M. *et al*. (1998) Increased microvascular density and enhanced leukocyte rolling and adhesion in the skin of VEGF transgenic mice. *J. Invest. Dermatol.*, **111**, 1–6.
6. Surazynski,A. *et al*. (2008) Extracellular matrix and HIF-1 signaling: the role of prolidase. *Int. J. Cancer*, **122**, 1435–1440.
7. Forsythe,J.A. *et al*. (1996) Activation of vascular endothelial growth factor gene transcription by hypoxia-inducible factor 1. *Mol. Cell. Biol.*, **16**, 4604–4613.
8. Olsson,A.K. *et al*. (2006) VEGF receptor signalling—in control of vascular function. *Nat. Rev. Mol. Cell Biol.*, **7**, 359–371.
9. Liao,D. *et al*. (2007) Hypoxia: a key regulator of angiogenesis in cancer. *Cancer Metastasis Rev.*, **26**, 281–290.
10. Iyer,N.V. *et al*. (1998) Cellular and developmental control of O2 homeostasis by hypoxia-inducible factor 1 alpha. *Genes Dev.*, **12**, 149–162.
11. Ryan,H.E. *et al*. (1998) HIF-1 alpha is required for solid tumor formation and embryonic vascularization. *EMBO J.*, **17**, 3005–3015.
12. Strieter,R.M. (2005) Masters of angiogenesis. *Nat. Med.*, **11**, 925–927.
13. Li,Y. *et al*. (2006) UVB radiation induces expression of HIF-1alpha and VEGF through the EGFR/PI3K/DEC1 pathway. *Int. J. Mol. Med.*, **18**, 713–719.
14. Jiang,B.H. *et al*. (2008) AKT signaling in regulating angiogenesis. *Curr. Cancer Drug Targets*, **8**, 19–26.
15. Surh,Y.J. (2003) Cancer chemoprevention with dietary phytochemicals. *Nat. Rev. Cancer*, **3**, 768–780.
16. Hakkinen,S.H. *et al*. (1999) Content of the flavonols quercetin, myricetin, and kaempferol in 25 edible berries. *J. Agric. Food Chem.*, **47**, 2274–2279.
17. Ribeiro de Lima,M.T. *et al*. (1999) Determination of stilbenes (trans-astringin, cis- and trans-piceid, and cis- and trans-resveratrol) in Portuguese wines. *J. Agric. Food Chem.*, **47**, 2666–2670.
18. Sellappan,S. *et al*. (2002) Flavonoids and antioxidant capacity of Georgia-grown Vidalia onions. *J. Agric. Food Chem.*, **50**, 5338–5342.
19. Lu,J. *et al*. (2006) Inhibition of Mammalian thioredoxin reductase by some flavonoids: implications for myricetin and quercetin anticancer activity. *Cancer Res.*, **66**, 4410–4418.
20. Lee,K.W. *et al*. (2007) Myricetin is a novel natural inhibitor of neoplastic cell transformation and MEK1. *Carcinogenesis*, **28**, 1918–1927.
21. Ko,C.H. *et al*. (2005) Myricetin inhibits matrix metalloproteinase 2 protein expression and enzyme activity in colorectal carcinoma cells. *Mol. Cancer Ther.*, **4**, 281–290.
22. Jung,S.K. *et al*. (2008) Myricetin suppresses UVB-induced skin cancer by targeting Fyn. *Cancer Res.*, **68**, 6021–6029.
23. Ding,M. *et al*. (2006) Cyanidin-3-glucoside, a natural product derived from blackberry, exhibits chemopreventive and chemotherapeutic activity. *J. Biol. Chem.*, **281**, 17359–17368.
24. Albini,A. *et al*. (2005) Tumor inflammatory angiogenesis and its chemoprevention. *Cancer Res.*, **65**, 10637–10641.
25. DeLisser,H.M. *et al*. (1997) Involvement of endothelial PECAM-1/CD31 in angiogenesis. *Am. J. Pathol.*, **151**, 671–677.
26. DiMaio,T.A. *et al*. (2008) PECAM-1 isoform-specific functions in PECAM-1-deficient brain microvascular endothelial cells. *Microvasc. Res.*, **75**, 188–201.
27. Harris,A.L. (2002) Hypoxia–a key regulatory factor in tumour growth. *Nat. Rev. Cancer*, **2**, 38–47.
28. Miyoshi,A. *et al*. (2006) Hypoxia accelerates cancer invasion of hepatoma cells by upregulating MMP expression in an HIF-1alpha-independent manner. *Int. J. Oncol.*, **29**, 1533–1539.
29. Mylonis,I. *et al*. (2006) Identification of MAPK phosphorylation sites and their role in the localization and activity of hypoxia-inducible factor-1 alpha. *J. Biol. Chem.*, **281**, 33095–33106.
30. Gao,N. *et al*. (2004) Arsenite induces HIF-1alpha and VEGF through PI3K, Akt and reactive oxygen species in DU145 human prostate carcinoma cells. *Mol. Cell. Biochem.*, **255**, 33–45.
31. Hanahan,D. *et al*. (1996) Patterns and emerging mechanisms of the angiogenic switch during tumorigenesis. *Cell*, **86**, 353–364.
32. Nijsten,T. *et al*. (2004) Cyclooxygenase-2 expression and angiogenesis in squamous cell carcinoma of the skin and its precursors: a paired immunohistochemical study of 35 cases. *Br. J. Dermatol.*, **151**, 837–845.
33. Newell,B. *et al*. (2003) Comparison of the microvasculature of basal cell carcinoma and actinic keratosis using intravital microscopy and immunohistochemistry. *Br. J. Dermatol.*, **149**, 105–110.
34. Li,V.W. *et al*. (2008) Antiangiogenesis in the treatment of skin cancer. *J. Drugs Dermatol.*, **7**, s17–s24.
35. Tosetti,F. *et al*. (2002) Angioprevention: angiogenesis is a common and key target for cancer chemopreventive agents. *FASEB J.*, **16**, 2–14.
36. Mukhtar,H. *et al*. (1988) Exceptional activity of tannic acid among naturally occurring plant phenols in protecting against 7,12-dimethylbenz(a)anthracene-, benzo(a)pyrene-, 3-methylcholanthrene-, and N-methyl-N-nitrosourea-induced skin tumorigenesis in mice. *Cancer Res.*, **48**, 2361–2365.
37. Claffey,K.P. *et al*. (1996) Expression of vascular permeability factor/vascular endothelial growth factor by melanoma cells increases tumor growth, angiogenesis, and experimental metastasis. *Cancer Res.*, **56**, 172–181.
38. Graeven,U. *et al*. (2000) Expression patterns of placenta growth factor in human melanocytic cell lines. *J. Invest. Dermatol.*, **115**, 118–123.
39. Carmeliet,P. *et al*. (1996) Abnormal blood vessel development and lethality in embryos lacking a single VEGF allele. *Nature*, **380**, 435–439.
40. Ferrara,N. *et al*. (1996) Heterozygous embryonic lethality induced by targeted inactivation of the VEGF gene. *Nature*, **380**, 439–442.
41. Stetler-Stevenson,W.G. (2008) The tumor microenvironment: regulation by MMP-independent effects of tissue inhibitor of metalloproteinases-2. *Cancer Metastasis Rev.*, **27**, 57–66.
42. Bergers,G. *et al*. (2000) Matrix metalloproteinase-9 triggers the angiogenic switch during carcinogenesis. *Nat. Cell Biol.*, **2**, 737–744.
43. Handsley,M.M. *et al*. (2005) Metalloproteinases and their inhibitors in tumor angiogenesis. *Int. J. Cancer*, **115**, 849–860.
44. Stearns,M.E. *et al*. (1999) Interleukin 10 (IL-10) inhibition of primary human prostate cell-induced angiogenesis: IL-10 stimulation of tissue

inhibitor of metalloproteinase-1 and inhibition of matrix metalloproteinase (MMP)-2/MMP-9 secretion. *Clin. Cancer Res.*, **5**, 189–196.
45. Swinson,D.E. *et al*. (2004) Hypoxia-inducible factor-1 alpha in non small cell lung cancer: relation to growth factor, protease and apoptosis pathways. *Int. J. Cancer*, **111**, 43–50.
46. Clottes,E. (2005) [Hypoxia-inducible factor 1: regulation, involvement in carcinogenesis and target for anticancer therapy]. *Bull. Cancer*, **92**, 119–127.
47. Treins,C. *et al*. (2002) Insulin stimulates hypoxia-inducible factor 1 through a phosphatidylinositol 3-kinase/target of rapamycin-dependent signaling pathway. *J. Biol. Chem.*, **277**, 27975–27981.
48. Semenza,G.L. (2003) Targeting HIF-1 for cancer therapy. *Nat. Rev. Cancer*, **3**, 721–732.
49. Richard,D.E. *et al*. (1999) p42/p44 mitogen-activated protein kinases phosphorylate hypoxia-inducible factor 1alpha (HIF-1alpha) and enhance the transcriptional activity of HIF-1. *J. Biol. Chem.*, **274**, 32631–32637.
50. Walker,E.H. *et al*. (2000) Structural determinants of phosphoinositide 3-kinase inhibition by wortmannin, LY294002, quercetin, myricetin, and staurosporine. *Mol. Cell*, **6**, 909–919.

Received October 30, 2008; revised August 26, 2009; accepted September 3, 2009